Erythropoietin Promotes the Differentiation of Fetal Neural Stem Cells into Glial Cells Partly via EPOR-βCR/Syne-1/H3K9me3 Pathway

Sijia Zhang
Xuanwu Hospital, Capital Medical University
Rongliang Wang
Xuanwu Hospital, Capital Medical University
Fangfang Li
Xuanwu Hospital, Capital Medical University
Zhen Tao
Xuanwu Hospital, Capital Medical University
Zhenhong Yang
Xuanwu Hospital, Capital Medical University
Haiping Zhao
Xuanwu Hospital, Capital Medical University
Yumin Luo (yumin111@ccmu.edu.cn)
Xuanwu Hospital, Capital Medical University

Research

Keywords: EPO, hypoxia, neural stem and progenitor cells, β common receptor

Posted Date: July 6th, 2020

DOI: https://doi.org/10.21203/rs.3.rs-39956/v1

Abstract

Erythropoietin (EPO) treatment has achieved a remarkable improvement of cognition in neonatal hypoxic-ischae mic encephalopathy (HIE) in clinical settings, however, it did not lower the severe neurodevelopmental impairment to extremely preterm infants, however, the primary cause of this discrepant phenomenon is still puzzling. Here, we explore the effect of EPO on post-hypoxic neurogenesis using fetal neural stem cells (NSCs)/neural progenitors (NPs) and whether the effect is mediated by EPOR/βCR heteromimer. Fetal NSCs/NPs was treated with EPO at different time point after oxygen and glucose deprivation/reoxygenation (OGD/R). Cell viability, proliferation, and differentiation of NSCs/NPs were detected by CellTiter-Glo, Edu assay, flow cytometry and RT-PCR. We found that EPO treatment at different time point increased the cell viability without affecting the proliferation. EPO treatment immediately after OGD/R promoted the oligodendrocyte and astrocyte differentiation, while decreased neuronal differentiation of NSCs/NPs. Furthermore, immunofluorescence and co-immunoprecipitation proved the existence of EPOR/βCR heterodimer on NSCs/NPs, and EPO treatment significantly increase the mRNA expression of βCR and elevated the correlation between levels of EPOR and βCR. Moreover, EPOR and βCR receptors were both correlated with markers of oligodendrocytes. In addition, mass spectrometer analysis identified Syne-1 as one downstream signaling of EPOR/βCR heterodimer. Immunofluorescence and western blot indicated that βCR/Syne-1/H3K9me3 pathway was possibly involved in the function of EPO. Collectively, our data revealed that EPO treatment immediately after OGD/R was not a good time point for neurogenesis, and EPO could promote the formation of EPOR/βCR on fetal NSCs/NPs which mediates its function on glia differentiation.

1 Introduction

Hypoxic-ischaemic encephalopathy (HIE) causes dramatic brain damage in early life and resulted in serious impairment to brain development. Erythropoietin (EPO) is a cytokine mainly induced under hypoxic conditions, which primarily acts on the erythroid progenitor cells in the bone marrow. Compelling evidences have revealed its secondary functions, with a crucial focus on the central nervous system. However, differences exist in the regulatory effects of EPO on the differentiation of neurons at different stages of brain development. Clinical trials had shown that exogenous EPO causes reduction in death and better long term neuro-developmental outcome in neonatal HIE both singly or as an adjuvant to therapeutic hypothermia [1]. Similarly, high-dose EPO administration prompts newly differentiating neurons in the adult mouse brain [2]. Instead, it was recently showed that high-dose EPO treatment administered to extremely preterm infants from 24 hours after birth through 32 weeks of postmenstrual age did not result in a lower risk of severe neurodevelopmental impairment or death at 2 years of age [3]. Nevertheless, the primary cause of this discrepant phenomenon is still puzzling.

EPO may interact with up to four distinct isoforms of its receptor (homodimers EPOR/EPOR or hetero-oligomers EPOR/βCR), activating different signaling cascades with roles in neuroprotection and neurogenesis. It was demonstrated that high-dose EPO administration, amplify auto/paracrine EPO/EPOR signaling, prompts the emergence of new CA1 neurons and enhanced dendritic spine densities [2]. Even if the presence of all these different isoforms paves the way for new interesting mechanisms through which

EPO could exert its function in the brain, many questions remain unanswered. Indeed, it is necessary to investigate how EPO's binding to each isoform activates a specific intracellular pathway, modulating the expression of target genes. Once these mechanisms have been elucidated, it will be possible to develop new isoform-selective drugs, resulting in a more specific therapy. However, a direct interaction between the EPOR and the βCR to form an innate repair receptor is controversial [4], and until now, whether the present of EPOR/βCR heterodimer on neural stem cells (NSCs)/neural progenitors (NPs) and whether it mediates the neurogenesis effect of EPO remain unknown.

In the present study, we make use of primary cortical NSCs/NPs from fetus mouse to explore the effect of EPO intervention on neurogenesis in vitro at different time points after reoxygenation and the possible mechanism to provide some foundation for the future basic research and the clinical trial of HIE.

2 Materials And Methods

2.1 Culture of primary neural stem cells (NSCs) and neural progenitors (NPs)

Female C57BL/6 mice (25 g-30 g, 2-month-old) were purchased from SPF (Beijing) Biotechnology Co.,Ltd. and approved by the Institutional Animal Care and Use Committee of Capital Medical University. Cortex from embryonic day 14 (E14) mice were isolated and minced in a 0.25% trypsin solution for 5 min at 37 °C. The tissue was washed in media containing 10% FBS, and then passed through a 70 μm cell strainer. The extracted cells were resuspended in complete medium containing DMEM/F12, neurobasal, 2% B27, 10 ng/mL EGF, 10 ng/mL bFGF, 1% GlutaMAX and 1% penicillin/streptomycin, plated in Ultra Low Attachment six well Plates, and maintained at 37 °C in a humidified atmosphere containing 5% CO_2. NSCs and NPs were subcultured by accutase every 2–3 days. The third passage cells were plated onto PDL–coated cell culture plates with complete medium.

2.2 Oxygen and glucose deprivation (OGD) operation

Cell medium was replaced by glucose-free Dulbecco's modified Eagles medium (DMEM) (Gibco; Thermo Fisher Scientific, Inc.) in a a three-gas incubator containing 95% nitrogen and 5% CO_2 at 37 °C for 1, 2, 4, 6, 8 h, respectively. Then cells were switched to glucose-containing medium and maintained at 37 °C, 5% CO2 incubator for 1, 2, 4, 7 days, respectively.

2.3 Cell viability assay

Cell viability was assessed by the CellTiter-Glo®Luminescent Cell Viability Assay. Briefly, equilibrate the plate and its contents at room temperature for approximately 30 minutes, then add a volume of CellTiter-Glo®Reagent equal to the volume of cell culture medium present in each well and mix contents for 2 minutes on an orbital shaker to induce cell lysis. Allow the plate to incubate at room temperature for 10 minutes to stabilize luminescent signal, and record luminescence with the luminometer.

2.4 EdU incorporation assay

Proliferation of NSCs and NPs was assessed by Click-iT® EdU Imaging Kits according to the manufacturer's instructions. Isolated NSCs and NPs were seeded on 48-well-plates (4×10^5 cells/well) and cultured in medium without EGF and bFGF. After OGD operation, EdU was added to the medium and cells were cultured for another 4 days. Cultured cells were fixed with 4% PFA for 15 min, followed by permeabilization step using 0.5% Triton X-100. After permeabilization, the cells were incubated with Click-iT® reaction cocktails for 30 min in dark room. The number of total cells and Edu-positive cells were mounted using high content analysis.

2.5 Flow cytometry for assessment of EGFR and DCX

Neurospheres were dissociated by Accutase (Sigma). Select a fraction of cells from each tube to prepare a negative control tube (unmarked cells). Cells were fixed with 4% PFA for 30 minutes followed by wash with 1 ml PBS 0.15% BSA and incubation with 0.5% Triton X-100 for 30 minutes. Cells were washed once with 1 ml PBS 0.15% BSA and incubated with EGFR Antibody (Alexa Fluor® 750, Novus) or Doublecortin antibody (PE, biorbyt) for 30 minutes in dark. Cells were washed once and resuspended in PBS. Cells were then analysised on a BD FACSCalibur.

2.6 Real-time reverse transcription PCR (RT-PCR)

Purified RNA from NSCs and NPs were used as a template to synthesize cDNA using oligo-d (T) primers and SuperScript III /RNaseOUT Enzyme Mix (Invitrogen, Carlsbad, CA, USA). Relative gene expression was calculated *via* the $2 - \Delta\Delta CT$ method, normalized, and expressed as fold change relative to U6 or β-actin. RT-PCR was performed in triplicate. Primers for myelin basic protein (*Mbp*): F: 5'-TCCGACGAGCTTCAGACCA-3', R: 5'-ACCCCTGTCACCGCTAAAGA-3'; primers for 2',3'-cyclic nucleotide 3'-phosphodiesterase (*CNPase*): F:5'-GCCTTCAAGAAAGAGCTTCG-3'; R: 5'-CAGATCACTGGGCCACAACT-3'; primers for microtubule associated protein-2 (*Map-2*): F: 5'-TCTCTAAAGAACATCCGTCAC-3', R: 5'-ATCTTCACATTACCACC TCC-3'; primers for β-tubulin-III (*Tubb3*) F:5' GCGCCTTTGGACACCTATT-3', R:5'-CCAGCACCACTCTGACCAA-3'; primers for glial fibrillary acidic protein (*Gfap*): F: 5'-AACAACCTGGCTGCGTAT-3', R: 5'-CTGCCTCGTATTGAGTGC-3'; primers for S100 calcium binding protein B (*S100b*): F:5'-CCCTCATTGATGTCTTCCACC3', R:5'-TTCCTGCTCCTTGATTTCCTC-3'; primers for *Epor* F:5'-TCCTGGAGCACCTAT GACC-3', R:5'-CGAGATGAGGACCAGAATGA-3'; primers for βcr (*Csf2rb*) F:5'-TGGAGCAAGTGGAGCGAA-3', R:5'-CACAGCCAAAGCGAAGGAT-3'.

2.7 Co-Immunoprecipitation (Co-IP)

Co-IP assays were performed to identify the proteins. Briefly, 1×10^6 cells were collected and lysed in 300μL buffer containing nondenaturing lysis buffer, protease inhibitor and phosphatase inhibitors. For Co-IP using antibodies, before being added to the cell lysates, the antibodies were incubated with Protein A/G Magnetic Beads (Sigma-Aldrich) and IgG for 3 h at 4 °C to eliminate nonspecific binding. Then, the crosslinked Protein A/G Magnetic Beads were added to the cell lysates directly and incubated overnight at 4 °C. The magnetic beads were washed with IP wash buffer and collected. The protein complexes were eluted from the beads by 50 mM glycine (pH 2.8) and analyzed by Western blot.

2.7 Liquid chromatography tandem mass spectrometry (LC-MS/MS)

Protein bands were excised from the SDS-PAGE gels and were dissolved with 50 μl mobile phase A (H_2O, 0.1% formic acid) and loaded onto a Acclaim PePmap C18-reversed phase column (75μm × 2 cm, 3 μm, 100 Åthermo scientific) and separated with reversed phase C18 column (75μm × 10 cm, 5 μm, 300 Å Agela Technologies) mounted on a Dionex ultimate 3000 nano LC system. Peptides were eluted using a gradient : Start from 5% Buffer B ; 0 ~ 6 min 5%~8% Buffer B; 6 ~ 40 min 8–30% Buffer B; 40 ~ 45 min 30–60% Buffer B, 45–48 min 60–80% Buffer B; 48–56 min 80% Buffer B; 56–58 min increasing to 5% Buffer B; 58–65 min 5% Buffer B.at a flow rate of 400 nL min-1 combined with a Q Exactive mass spectrometer Thermo Fisher Scientific, Waltham, MA, USA). The eluates were directly entered Q–Exactive MS (Thermo Fisher Scientific), setting in positive ion mode and data-dependent manner with full MS scan from 350–2000 m/z, full scan resolution at 70,000, MS/MS scan resoltion at 17,500. MS/MS scan with minimum signal threshold 1E + 5, isolation width at 2 Da. To evaluate the performance of this mass spectrometry on the samples, two MS/MS acquisition modes, higher collision energy dissociation (HCD) was employed. And to optimize the MS/MS acquisition efficiency of HCD, normalized collision energy (NCE) was systemically examined 28%.

2.8 Western blot

Cell samples were processed for Western blot analysis as previously described. The PVDF membranes (Millipore corporation, MA, USA) were incubated with following primary antibodies at 4 °C overnight: anti-EPOR (rabbit, orb164257, Biorbyt, 1:1000), anti-βCR (mouse, 393281, Santa, 1:1000), anti-H3K9me3 (mouse, 5327, CST, 1:100). Antigen-antibody complexes were observed by enhanced chemiluminescence using an Immobilon Western blotting kit. The intensity of the bands was detected using a FluorChem®HD2 Gel Imaging System (Protein Simple, USA). The gray value of bands was analyzed by AlphaEase FC software (Alpha Innotech, CA, USA).

2.9 βCR siRNA transfection

NSCs and NPs were transfected with βCR siRNA using Lipofectamine Stem Transfection Reagent (Invitrogen, Carlsbad, CA, USA) for 48 h according to the manufacturer's instructions and the transfection efficiency was validated by western blot.

2.10 Immunofluorescence analysis

Cells were fixed using 4% PFA for 15 min. After being washed three times in PBS, they were incubated with 3% BSA for 1 h. Cells were immunostained with primary antibodies of anti-EPOR (rabbit, orb164257, Biorbyt, 1:100), anti-βCR (mouse, 393281, Santa, 1:100), anti-H3K9 (mouse, 5327, CST, 1: 100) and anti-Syne-1 (rabbit, ab192234, abcam, 1:100). After incubating with secondary antibodies conjugated with DyLight 488 or Cy3 (Jackson ImmunoResearch), cells were counterstained with DAPI. The images were digitized using an Olympus Fluoview FV1000 microscope (Olympus, Japan).

2.11 Statistical analysis

Statistical analysis was performed using SPSS 23.0 software. Numeric data are presented as the mean standard deviation. Student's t test was used for two-group comparisons. One-way ANOVA with Tukey–Kramer post hoc test was used for comparisons among several quantitative variables. The correlation between two variables was assessed using Pearson's correlation test. Data for neurobehavioral tests were analyzed by a two-way repeated measures (RM) ANOVA followed by the Bonferroni post hoc correction. The correlation between two variables was performed using the Pearson's correlation test. $P < 0.05$ was considered statistically significant.

3 Results

3.1 OGD time-dependently depressed neurogenesis of NSCs/NPs by decreasing cell proliferation and viability

To mimic the pathological change of HIE, we isolated cerebral cortical NSCs/NPs from fetus mouse and established the OGD model, and investigate the direct effect of hypoxic injury on the proliferation rate and cell viability of NSCs/NPs by Edu incorporation and CellTiter-Glo cell viability assay. The results indicated that OGD significantly reduced both proliferation (Fig. 1a, c, $P < 0.05$) and cell viability (Fig. 1b, $P < 0.05$) of NSCs/NPs. Furthermore, the cell viability decreased continuously with the extension of hypoxic time (Fig. 1b, $P < 0.05$), while the decrease of cell proliferation experienced a plateau from 2 h to 6 h (Fig. 1a, $P < 0.05$), suggesting that the 2 h to 6 h might be mild duration time of the OGD model on the NSCs/NPs. In summary, we proved that the hypoxia damaged neurogenesis partly via decreasing cell viability and proliferation.

3.2 EPO treatment at different time point after OGD/R rescued cell viability rather than proliferation of NSCs/NPs

Next we explored the effect of EPO on the proliferation rate and cell viability of cortical NSCs/NPs after OGD 2 h and 6 h, representing mild and severe hypoxic injury. We showed that EPO administration at 1 h to 6 h after OGD 2 h or 6 h could increase the survival of NSCs/NPs (Fig. 2a, 2b, $P < 0.05$), with no effect on the proliferation rate (Fig. 2c, 2d). Moreover, we detected EGFR% by flow cytometry to compare the ratio of actively proliferating cells among 2 h OGD group, immediate EPO treament after OGD (EPO immediately) group and delayed EPO treament (EPO 1 h) group. The results indicated the ratio of EGFR positive cells were almost no difference among cells in the three groups 24 h after OGD (Fig. 2e). Therefore, immediate or delayed delivery of EPO could promote neural regeneration after hypoxic injury by increasing cell viability without influencing cell proliferation.

3.3 EPO treatment immediately after OGD/R boosted the differentiation of NSCs/NPs towards oligodendrocytes and astrocytes

Differentiation of NSCs/NPs to neurons, oligodendrocytes and astrocytes is another key process during neurogenesis. Firstly we explore the differentiation towards neurons. We detected DCX% by flow cytometry to compare the differentiation to neurons among 2 h OGD group, immediate EPO treament after OGD (EPO immediately) group and delayed EPO treament (EPO 1 h) group at 1 day after OGD1h, 2 h, 4 h, 6 h, 8 h (Fig. 3a). To our surprise, when treated immediately, EPO decreased the DCX%, indicating the inhibition of EPO on differentiation towards neurons (Fig. 3a, $P < 0.05$), while EPO treament 1 h after OGD didn't alter the ratio of DCX positive cells, suggesting delayed delivery of EPO exert no effect on differentiation of NSCs/NPs towards neurons. Furthermore, by detecting the relative mRNA level of MAP-2 and β-tublin, two markers for mature neurons, at 7 day after OGD, we found that OGD and immediate EPO treament didn't significantly alter the potential of NSCs/NPs differentiate to neurons (Fig. 3b).

We further detected the effect of immediate EPO treament on glial differentiation of NSCs/NPs. We demonstrated that OGD from 1 h to 8 h didn't significantly change the relative mRNA levels of MBP and CNPase, two markers of mature oligodendrocytes, at 7 day after OGD, suggesting that the differentiation towards oligodendrocytes may not be directly affected by hypoxia. However, the relative mRNA levels of both MBP and CNPase were significantly elevated after EPO administration, which suggested that EPO could promote the oligodendrocyte regeneration (Fig. 3c, $P < 0.05$). The mRNA level of GFAP, a marker for mature astrocytes, was significantly increased by EPO treatment. Another marker for astrocytes, S100β, was also slightly increased by EPO treament in OGD 1 h, 4 h, 6 h, and 8 h groups, indicating that EPO could also promote the differentiation towards astrocytes (Fig. 3d, $P < 0.05$). In summary, EPO treatment immediately after reoxygenation promoted the differentiation of NSCs/NPs towards oligodendrocytes and astrocytes but not neurons.

3.4 EPOR/βCR heteromimer exists on NSCs/NPs

To determine the existence of EPOR homodimers or hetero-oligomers on the surface of NSCs/NPs, immunofluorescence, confocal microscopy and Co-IP were used. We first identified that both EPOR/EPOR homodimer and EPOR/βCR hetero-oligomers exists on the NSCs/NPs (Fig. 4a). Furthermore, Co-IP indicated that EPOR and βCR were bound together in NSCs/NPs in control, OGD and EPO treatment group (Fig. 4b). In addition, EPO treatment did not influence the mRNA levels of Epor (Fig. 4d), but increased the expression of βcr in NSCs and NPs compared with control group (Fig. 4c, $P < 0.05$), while. By correlation analysis, we found that the mRNA levels of βcr was positively correlated with the mRNA levels of Epor when cells were given EPO treament after OGD (Fig. 4f, $P < 0.05$), while cells without EPO treatment after OGD showed no significant correlation between Epor and βcr (Fig. 4e). In summary, we preliminary proved the existence of EPOR/βCR heterodimer on the surface of NSCs/NPs, and EPO treatment significantly increase the mRNA expression of βCR and elevated the correlation between levels of EPOR and βCR.

3.5 EPOR and βCR receptors were both correlated with markers of oligodendrocytes

To establish the preliminary link between the EPOR/βCR hetero-oligomers and the neural cell markers, we conducted the correlation analysis between the mRNA level of cell markers and the two receptors of EPO.

The results indicated that EPOR was positively correlated with the expression of GFAP, CNPase and MBP (Fig. 5b, 5c, $P < 0.05$), while βCR was positively correlated with the expression of MAP-2 and β□-tublin (Fig. 5d, $P < 0.05$), and CNPase (Fig. 5e). Our results suggest that EPOR might be involved in the differentiation of NSCs/NPs to mature oligodendrocytes and astrocytes, while βCR was possibly related to the differentiation of NSCs/NPs to mature neurons and oligodendrocytes. Therefore, the expression of EPOR and βCR receptors were both correlated with the expression of markers of oligodendrocytes.

3.6 Syne-1 (Nesprin) binds to EPOR/βCR heteromimer

To explore the possible downstream signaling pathways of EPOR/βCR hetero-oligomers, LC-MS/MS was used to analyze the EPOR-interacting proteins (Fig. 6a). Two protein bands were pulled down by the EPOR antibody after non-specific binding proteins were removed by IgG and Protein A/G magnetic beads (Fig. 6b) and performed LC-MS/MS analysis. We identified 50 and 60 potential EPOR-binding proteins from OGD and EPO treated cells, respectively. Venn analysis showed that 32 of these proteins were commonly found in two groups of cells (Fig. 6c), and 18 and 28 proteins were found only in OGD and EPO treated cells (Table 1). Besides, there were 5 potential proteins which were oxidized (Table 2) and another 5 potential proteins which were phosphorylated (Table 3) in the EPO treated cells. In sum, we identified 37 kinds of potential proteins that were expressed or chemically modified by EPO treatment, with one potential protein, Syne-1, which was both among the 28 proteins found only in EPO treated cells and phosphorylated by EPO treatment (Fig. 6d, 6e). Among them, we speculated Syne-1 as a key molecule for the effect of EPO on the oligodendrocytes differentiation of NSCs/NPs based on previous researches [5]. Since Syne-1 was found binding to EPOR, and further confocal immunofluorescence showed that Syne-1 was colocalized with βCR on the NSCs/NPs (Fig. 6f), suggesting Syne-1 was a potential downstream signaling of EPOR/βCR heteromimer.

Table 1
Proteins which were found only in EPO treated cells.

Gene name	Descripion	Mass	Score	Matches	Sequence	emPAI	Coverage
Actg2	Actin, gamma-enteric smooth muscle (Fragment) OS = Mus musculus OX = 10090 GN = Actg2 PE = 3 SV = 1	22158	60	3(2)	1(1)	0.15	8%
Tuba1a	Tubulin alpha-1A chain OS = Mus musculus OX = 10090 GN = Tuba1a PE = 1 SV = 1	50788	49	6(3)	4(2)	0.13	12%
Ralgapb	Ral GTPase-activating protein subunit beta OS = Mus musculus OX = 10090 GN = Ralgapb PE = 1 SV = 1	168180	22	14(0)	3(0)	0.02	0%
Eif4g1	Eif4g1 protein (Fragment) OS = Mus musculus OX = 10090 GN = Eif4g1 PE = 2 SV = 1	93878	15	2(0)	2(0)	0.03	2%
Syne1	Nesprin-1 OS = Mus musculus OX = 10090 GN = Syne1 PE = 1 SV = 1	1016647	26	9(1)	6(1)	0	0%
Fgf10	Fibroblast growth factor 10 OS = Mus musculus OX = 10090 GN = Fgf10 PE = 2 SV = 1	24095	23	2(0)	1(0)	0.14	3%
Pde11a	Dual 3',5'-cyclic-AMP and -GMP phosphodiesterase 11A OS = Mus musculus OX = 10090 GN = Pde11a PE = 1 SV = 1	105523	21	1(0)	1(0)	0.03	1%

Note: Mass: protein molecular weight; Score: protein score; Matches: the total number of matched peptides; Sepuence: the total number of sequences matched; emPAI: $10^{(\text{N observed/N observable})-1}$; Coverage: Protein identification coverage

Gene name	Descripion	Mass	Score	Matches	Sequence	emPAI	Coverage
Igkv4-92	Immunoglobulin kappa variable 4–92 (Fragment) OS = Mus musculus OX = 10090 GN = Igkv4-92 PE = 4 SV = 1	12882	17	1(0)	1(0)	0.27	13%
Cltc	Clathrin heavy chain OS = Mus musculus OX = 10090 GN = Cltc PE = 1 SV = 1	193631	81	4(2)	4(2)	0.03	3%
Atp1a2	Sodium/potassium-transporting ATPase subunit alpha OS = Mus musculus OX = 10090 GN = Atp1a2 PE = 1 SV = 1	104717	62	2(1)	2(1)	0.03	2%
Vdac3	Voltage-dependent anion-selective channel protein 3 OS = Mus musculus OX = 10090 GN = Vdac3 PE = 1 SV = 1	31175	47	1(1)	1(1)	0.11	4%
Plxna3	Plexin A3 OS = Mus musculus OX = 10090 GN = Plxna3 PE = 4 SV = 1	211361	41	5(1)	2(1)	0.02	0%
Pkm	Pyruvate kinase PKM (Fragment) OS = Mus musculus OX = 10090 GN = Pkm PE = 1 SV = 1	20809	39	1(1)	1(1)	0.16	5%
Top2b	DNA topoisomerase 2-beta OS = Mus musculus OX = 10090 GN = Top2b PE = 1 SV = 2	182707	34	5(1)	4(1)	0.02	2%
Dnajc8	DnaJ homolog subfamily C member 8 OS = Mus musculus OX = 10090 GN = Dnajc8 PE = 1 SV = 1	25819	26	2(0)	1(0)	0.13	5%

Note: Mass: protein molecular weight; Score: protein score; Matches: the total number of matched peptides; Sepuence: the total number of sequences matched; emPAI: $10^{(\text{N observed/N observable})-1}$; Coverage: Protein identification coverage

Gene name	Descripion	Mass	Score	Matches	Sequence	emPAI	Coverage
Nop56	Nucleolar protein 56 (Fragment) OS = Mus musculus OX = 10090 GN = Nop56 PE = 1 SV = 1	14164	24	6(0)	2(0)	0.24	11%
H2bc14	Histone H2B OS = Mus musculus OX = 10090 GN = H2bc14 PE = 1 SV = 1	13928	24	5(1)	2(1)	0.25	19%
Ap5z1	AP-5 complex subunit zeta-1 OS = Mus musculus OX = 10090 GN = Ap5z1 PE = 1 SV = 1	88721	22	3(0)	1(0)	0.08	1%
Try5	Peptidase S1 domain-containing protein OS = Mus musculus OX = 10090 GN = Try5 PE = 2 SV = 1	28002	18	2(0)	1(0)	0.12	7%
Cyp4a30b	Cytochrome P450, family 4, subfamily a, polypeptide 30b OS = Mus musculus OX = 10090 GN = Cyp4a30b PE = 3 SV = 1	58952	16	1(0)	1(0)	0.06	1%
Tspyl2	Testis-specific Y-encoded-like protein 2 OS = Mus musculus OX = 10090 GN = Tspyl2 PE = 1 SV = 1	77737	16	1(0)	1(0)	0.04	1%
Cfap57	Cilia- and flagella-associated protein 57 OS = Mus musculus OX = 10090 GN = Cfap57 PE = 1 SV = 3	145756	24	2(1)	2(1)	0.02	1%

Note: Mass: protein molecular weight; Score: protein score; Matches: the total number of matched peptides; Sepuence: the total number of sequences matched; emPAI: $10^{(\text{N observed/N observable})-1}$; Coverage: Protein identification coverage

Gene name	Descripion	Mass	Score	Matches	Sequence		emPAI	Coverage
Rp1l1	MCG56960 OS = Mus musculus OX = 10090 GN = Rp1l1 PE = 2 SV = 1	202299	23	2(0)	1(0)	0.02		0%
Ppp1r9a	Protein phosphatase 1, regulatory subunit 9A OS = Mus musculus OX = 10090 GN = Ppp1r9a PE = 1 SV = 1	109834	14	1(0)	1(0)	0.03		0%

Note: Mass: protein molecular weight; Score: protein score; Matches: the total number of matched peptides; Sepuence: the total number of sequences matched; emPAI: $10^{(\text{N observed/N observable})-1}$; Coverage: Protein identification coverage

Table 2
Proteins which were oxidized only in EPO treated cells.

Gene name	Descripion	Mass	Score	Matches	Sequence	emPAI	Coverage
Hba-x	Hemoglobin X, alpha-like embryonic chain in Hba complex (Fragment) OS = Mus musculus OX = 10090 GN = Hba-x PE = 1 SV = 1	18092	34	2(1)	2(1)	0.19	13%
Vim	Vimentin OS = Mus musculus OX = 10090 GN = Vim PE = 1 SV = 1	49220	60	4(2)	2(1)	0.07	5%
H2bc14	Histone H2B OS = Mus musculus OX = 10090 GN = H2bc14 PE = 1 SV = 1	13928	24	5(1)	2(1)	0.25	19%
Cyp4a30b	Cytochrome P450, family 4, subfamily a, polypeptide 30b OS = Mus musculus OX = 10090 GN = Cyp4a30b PE = 3 SV = 1	58952	16	1(0)	1(0)	0.06	1%
Atp5f1b	ATP synthase subunit beta, mitochondrial OS = Mus musculus OX = 10090 GN = Atp5f1b PE = 1 SV = 2	56265	82	2(2)	2(2)	0.12	4%

Note: Mass: protein molecular weight; Score: protein score; Matches: the total number of matched peptides; Sepuence: the total number of sequences matched; emPAI: $10^{(\text{N observed/N observable})-1}$; Coverage: Protein identification coverage

Table 3
Proteins which were oxidized only in EPO treated cells.

Gene name	Descripion	Mass	Score	Matches	Sequence	emPAI	Coverage
Ralgapb	Ral GTPase-activating protein subunit beta OS = Mus musculus OX = 10090 GN = Ralgapb PE = 1 SV = 1	168180	22	14(0)	3(0)	0.02	0%
Cyp4a30b	Cytochrome P450, family 4, subfamily a, polypeptide 30b OS = Mus musculus OX = 10090 GN = Cyp4a30b PE = 3 SV = 1	58952	16	1(0)	1(0)	0.06	1%
Syne1	Nesprin-1 OS = Mus musculus OX = 10090 GN = Syne1 PE = 1 SV = 1	1016647	26	9(1)	6(1)	0.00	0%
Hba-x	Hemoglobin X, alpha-like embryonic chain in Hba complex (Fragment) OS = Mus musculus OX = 10090 GN = Hba-x PE = 1 SV = 1	18092	34	2(1)	2(1)	0.19	13%
Fgf10	Fibroblast growth factor 10 OS = Mus musculus OX = 10090 GN = Fgf10 PE = 2 SV = 1	24095	23	2(0)	1(0)	0.14	3%

Note: Mass: protein molecular weight; Score: protein score; Matches: the total number of matched peptides; Sepuence: the total number of sequences matched; emPAI: $10^{(\text{N observed/N observable})-1}$; Coverage: Protein identification coverage

3.7 βCR receptor mediated Syne-1/H3K9 signaling downstream of EPO

According to previous researches, H3K9me3 was one of the downstream molecules of Syne-1 in oligodendrocyte progenitors and the methylation of H3K9 exerted important effect on the myelination and cell differentiation [5–7], thus we sought to investigate whether Syne-1/H3K9me3 was downstream signaling of EPOR/βCR heteromimer. The result of immunofluorescence staining showed that Syne-1 was decreased after OGD while EPO treatment increased Syne-1, which was reversed by βCR siRNA (Fig. 7a). Furthermore, western blot demonstrated that H3K9me3 was upregualted after OGD while was reduced by EPO treatment. Likewise, βCR siRNA reversed the effect of EPO on the H3K9me3 (Fig. 7b, 7c, $P < 0.05$).

Thus, EPO activate EPOR-βCR/Syne-1/H3K9me3 signaling pathway and control the cell fate switch of NSCs/NPs (Fig. 7d).

4 Discussion

The present study investigates the effect of EPO on the post-hypoxic neurogenesis using primary cortical NSCs/NPs of fetal mouse. We demonstrated that EPO treatment at different time points after OGD/R could promote the cell viability while exerts no significant effect on the cell proliferation. And EPO treatment immediately after OGD/R boosted the differentiation of NSCs/NPs towards oligodendrocytes and astrocytes. We also found that EPOR/βCR heteromimer exist on the cell surface of the fetal cortical NSCs/NPs, and Syne-1/H3K9me3 signaling pathway probably mediated the effect of EPOR-βCR heteromimer on oligodendrocytes. Collectively, our main contribution revealed that EPO treatment immediately after OGD/R was not a good time point for neurogenesis and the existence of EPOR/βCR heteromimer on fetal NSCs/NPs mediates its function on glia differentiation.

Perinatal hypoxic-ischemic encephalopathy (HIE) remains a major cause of morbidity and mortality. EPO is a prominent candidate. EPO has many effects on neurogenesis and oligodendrogenesis. However, in the present research we reported an unexpected result that EPO treatment to fetal cortical NSCs/NPs didn't induce any significant effect on its proliferation and differentiation into neurons, but increased the cell viability and their differentiation towards oligodendrocytes and astrocytes. The endogenous neurogenesis was far from enough to restore the damaged neurological function, which was partly due to the high apoptosis rate of NSCs/NPs [8]. And one mechanism of EPO on the generation of mature erythrocytes is to increase cell viability by activating the PI3K signaling pathway or Bcl-2 family [9, 10]. Previous studies suggested that EPO administration could increase proliferation and neuronal differentiation of normal NSCs/NPs [11]. Conversely, our results indicated that instead of cell proliferation and neuronal differentiation, EPO could promote the cell viability and differentiation towards oligodendrocytes and astrocytes of NSCs/NPs following OGD/R, which is partly common with previous results of Ehrenreich that EPO may be able to increase neurogenesis without entering cell cycle [12]. As it is known to all, white matter of CNS is composed of myelin and is derived from oligodendrocytes [13]. And hypoxia produces a rapid and significant loss of axons both in the acute phase and subacute period [14]. Spontaneous axonal regeneration is fundamental but inadequate to restore function. Therefore, our results show that EPO treatment immediately after OGD/R can not directly promote the differentiation of NSCs/NPs into neurons, but can reduce the axonal damage of neurons by promoting the differentiation of oligodendrocytes and astrocytes. Our data showed that EPO treatment immediately after OGD/R was not a good time point for neurogenesis, further demonstrated that the effects of EPO are dose- and timing-dependent in the hypoxic-injured brain.

Previous studies have demonstrated that EPOR/βCR exist on primary human renal epithelial cells, endothelial progenitor cells and macrophages [15–17]. Within the brain at least three versions of the EPO receptor are now known to exist, including the βCR [18]. While the heteromic EPO receptor involving the βCR was initially thought to confer neuroprotection, evidence now supports a role for this heteromic EPO receptor and the homodimeric EPO receptor in the protection of neurons and glia [18]. It was suggested that

nonpeptidyl compound STS-E412, a kind of EPO deprivate which selectively bind to EPOR/βCR heterodimer, could act as neuroprotective agents in the CNS, suggesting the neuroprotective role of EPOR/βCR heterodimer [15]. Our results demonstrated for the first time that EPOR/βCR heterodimer also exist on primary NSCs/NPs. Moreover, EPO treament could increased the mRNA level of βCR, and the correlation between EPOR and βCR. Different from our current findings, it was previously showed that EPOR's expression is induced by hypoxia and EPO, and its distribution corresponds to that of EPO, suggesting that brain EPO works in a paracrine/autocrine manner in response to hypoxia. While our data propose a possibility that EPO could promote the formation of EPOR/βCR heterodimer and the effect of EPO on NSCs/NPs was mediated by EPOR/βCR heterodimer. In addition, βCR was elevated by EPO treament, while the differentiation towards neurons was not altered by EPO, demonstrating there may be other ligands beside EPO that mediate the effect of βCR on neural differentiation, which need further research.

We also did correlation analysis to further identify the possible relationship between EPOR/βCR and differentiation of neural cells. EPOR was demonstrated to be related to oligodendrocytes markers, MBP and CNPase, as well as astrocyte marker GFAP, suggesting it might be involved in the oligodendrocytes and astrocytes differentiation. βCR was correlated to neuron markers β-tublin and MAP-2, and oligodendrocytes marker CNPase, suggesting that βCR was possibly involved in the neuron and oligodendrocytes differentiation. EPO treatment immediately after OGD/R boosted the differentiation of NSCs/NPs towards oligodendrocytes and astrocytes. Therefore, the expression of EPOR and βCR receptors were both correlated with the expression of markers of oligodendrocytes.

Better understanding of the progression of NSCs/NPs in the developing cerebral cortex is important for modeling neurogenesis. To further identify the downstream signaling of EPOR/βCR heterodimer, we analyzed the protein bands isolated by Co-IP with EPOR antibody, we found several kinds of proteins fragments that were likely to be involved in the effect of EPO on NSCs/NPs, among which Syne-1 (nesprins) might be related to oligodendrocytes differentiation [5]. As previous studies had discovered, Syne-1 are a family of multi-isomeric scaffolding proteins and form the linker of nucleoskeleton-and-cytoskeleton (LINC) with SUN (Sad1p/UNC84) proteins at the nuclear envelope. Syne-1 was exceptionally extensively expressed in the adult murine CNS and was known to regulate axon termination and synapse formation during neurodevelopment in the nervous system [19, 20]. The N-terminal cytosolic domain of Syne could act as a connection with C-terminal domain of cytosolic actin to interact with the nuclear periphery and with nucleosomal histone carrying repressive marks, indicating its important role in transducing signal into nucleus [21]. In the previous study, Histone-3 lysine 9 (H3K9) was demonstrated to be one of the downstream repressive histone of Syne-1 in the mouse oligodendrocyte progenitor differentiation [5]. H3K9 is known to be associated with pericentric heterochromatin and important in genomic stability and trimethylation at H3K9 (H3K9me3) is enriched in an adult neural stem cell niche [6]. H3K9me3 is enriched in genes associated with cellular maintenance and not expressed in axon/neuron generation [6], indicating that epigenetic modification (H3K9me3) was involved in cell fate transition. Various other studies also proved that H3K9 demethylation was related in cell differentiation [7]. Our results showed that the expression of H3K9me3 in the NSCs/NPs was increased after OGD treatment while EPO treatment could

decrease the level of H3K9me3, which might be associated in the effect of EPO on the oligodendrocyte differentiation of NSCs/NPs.

In summary, our results demonstrated that EPO treatment immediately after OGD/R could increase the cell viability and the differentiation towards oligodendrocytes of primary fetal mouse cortical NSCs/NPs. EPOR/βCR heterodimer and its downstream signaling pathway Syne-1/H3K9 was possibly involved in the effect of EPO on the oligodendrocyte differentiation of NSCs/NPs. We are aware that our results were not enough to draw the final conclusions of the effect and mechanism of EPO on the neurogenesis in HIE. The critical importance of animal experiments on the specific dose, timing, and frequency of EPO treatment prior to commencing clinical trials is evident.

Abbreviations

EPO, erythropoietin; HIE, hypoxic-ischae mic encephalopathy; NSCs, neural stem cells; NPs, neural progenitors; OGD/R, oxygen and glucose deprivation/reoxygenation; RT-PCR, real-time reverse transcription PCR; Co-IP, co-immunoprecipitation; LC-MS/MS, liquid chromatography tandem mass spectrometry; MBP, myelin basic protein; CNPase, 2',3'-cyclic nucleotide 3'-phosphodiesterase; MAP-2, microtubule associated protein-2; Tubb3, β-tubulin-III; GFAP, glial fibrillary acidic protein; S100β, S100 calcium binding protein B; βcr, colony stimulating factor 2 receptor, beta, low-affinity.

Declarations

Acknowledgement

This work was supported by the National Natural Science Foundation of China (81801149, 81471340, 81771412, and 81971222).

Author contribution

S.Z., R.W., F.L., Z.T., and Z.Y. conducted study design, experiments, data analysis, and manuscript preparation. Y.L. and H.Z. designed and managed the research.

Ethics approval

The animal procedures involved in this study were approved by Institutional Animal Care and Use Committee of the Capital Medical University.

Consent for publication

Not applicable.

Competing interests

The authors declare that they have no conflicts of interest.

Availability of data and materials

Please contact author for data requests.

Ethics approval and consent to participate

Not applicable.

References

1. Toriuchi K, et al. Prolonged astrocyte-derived erythropoietin expression attenuates neuronal damage under hypothermic conditions. J Neuroinflammation. 2020;17(1): 141.
2. Wakhloo D, et al. Functional hypoxia drives neuroplasticity and neurogenesis via brain erythropoietin. Nat Commun. 2020;11(1): 1313.
3. Juul SE, et al. A Randomized Trial of Erythropoietin for Neuroprotection in Preterm Infants. N Engl J Med. 2020;382(3): 233-243.
4. Cheung Tung Shing KS, et al. EPO does not promote interaction between the erythropoietin and beta-common receptors. Sci Rep. 2018;8(1): 12457.
5. Hernandez M, et al. Mechanostimulation Promotes Nuclear and Epigenetic Changes in Oligodendrocytes. J Neurosci. 2016;36(3): 806-813.
6. Jiang Y, et al. Setdb1-mediated histone H3K9 hypermethylation in neurons worsens the neurological phenotype of Mecp2-deficient mice. Neuropharmacology. 2011;60(7-8): 1088-1097.
7. Lu C, et al. IDH mutation impairs histone demethylation and results in a block to cell differentiation. Nature. 2012;483(7390): 474-478.
8. Arvidsson A, et al. Neuronal replacement from endogenous precursors in the adult brain after stroke. Nat Med. 2002;8(9): 963-970.
9. Motoyama N, et al. Massive cell death of immature hematopoietic cells and neurons in Bcl-x-deficient mice. Science. 1995;267(5203): 1506-1510.
10. Richmond TD, et al. Turning cells red: signal transduction mediated by erythropoietin. Trends Cell Biol. 2005;15(3): 146-155.
11. Chen ZY, et al. Endogenous erythropoietin signaling is required for normal neural progenitor cell proliferation. J Biol Chem. 2007;282(35): 25875-25883.
12. Hassouna I, et al. Revisiting adult neurogenesis and the role of erythropoietin for neuronal and oligodendroglial differentiation in the hippocampus. Mol Psychiatry. 2016;21(12): 1752-1767.

13. Baumann N, et al. Biology of oligodendrocyte and myelin in the mammalian central nervous system. Physiol Rev. 2001;81(2): 871-927.
14. Hinman JD. The back and forth of axonal injury and repair after stroke. Curr Opin Neurol. 2014;27(6): 615-623.
15. Miller JL, et al. Discovery and Characterization of Nonpeptidyl Agonists of the Tissue-Protective Erythropoietin Receptor. Mol Pharmacol. 2015;88(2): 357-367.
16. Bennis Y, et al. Priming of late endothelial progenitor cells with erythropoietin before transplantation requires the CD131 receptor subunit and enhances their angiogenic potential. J Thromb Haemost. 2012;10(9): 1914-1928.
17. Lee TS, et al. beta Common Receptor Mediates Erythropoietin-Conferred Protection on OxLDL-Induced Lipid Accumulation and Inflammation in Macrophages. Mediators Inflamm. 2015;2015(439759.
18. Ostrowski D, et al. Alternative Erythropoietin Receptors in the Nervous System. J Clin Med. 2018;7(2).
19. Zhou C, et al. Mouse models of nesprin-related diseases. Biochem Soc Trans. 2018;46(3): 669-681.
20. Tulgren ED, et al. The Nesprin family member ANC-1 regulates synapse formation and axon termination by functioning in a pathway with RPM-1 and beta-Catenin. PLoS Genet. 2014;10(7): e1004481.
21. Lombardi ML, et al. The interaction between nesprins and sun proteins at the nuclear envelope is critical for force transmission between the nucleus and cytoskeleton. J Biol Chem. 2011;286(30): 26743-26753.

Figures

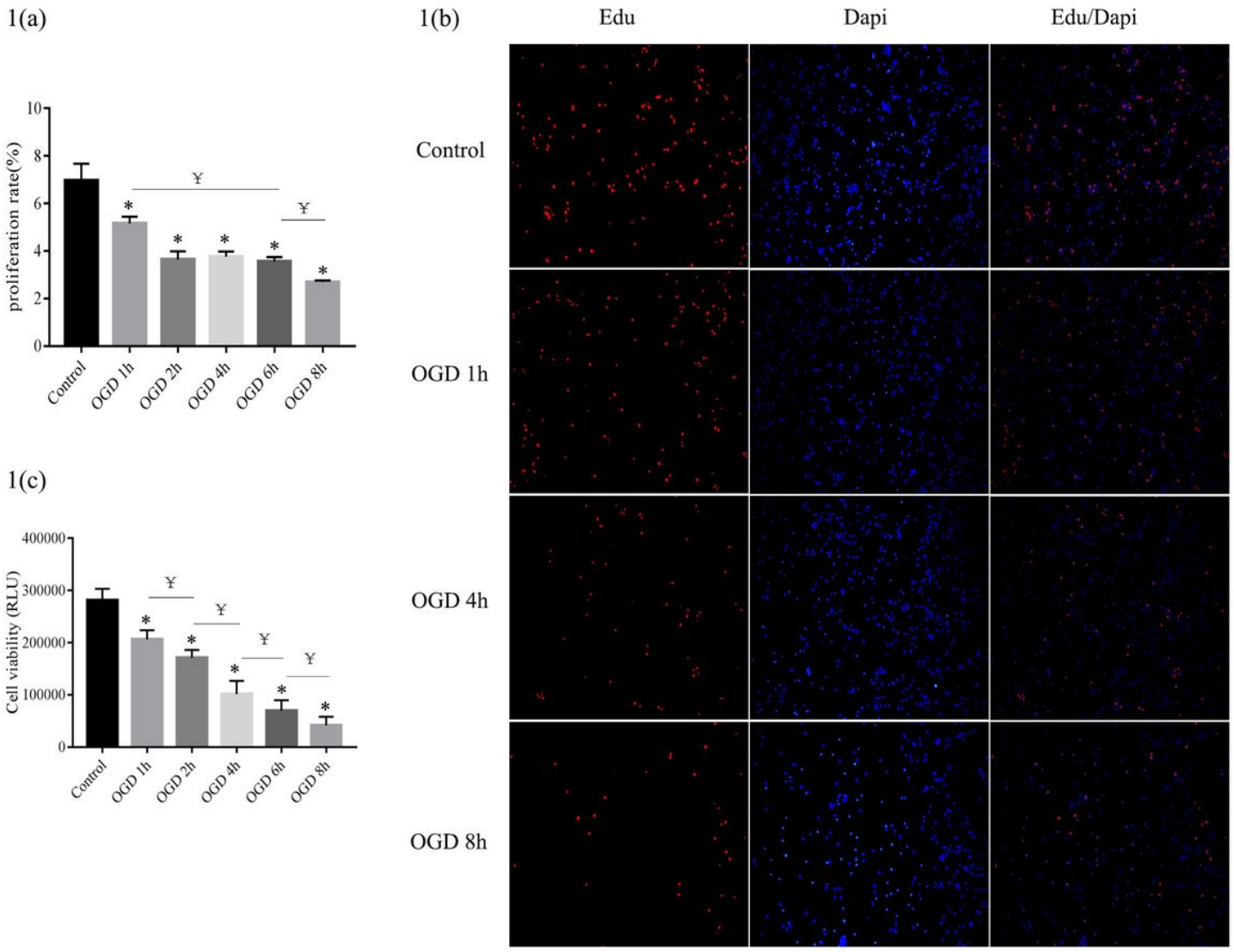

Figure 1

Cell proliferation and viability of neural stem and progenitor cells were decreased after oxygen-glucose deprivation/reoxygenation (OGD/R) treatment. (a, b) Proliferation rate was detected at OGD/R4d by Edu analysis. The positive (red) cells indicated activated proliferating cells. n=6/group. (c) Cell viability was measured at OGD/R2d by CellTiter-Glo®Luminescent assay. n=8/group. Control, OGD1h, 2h, 4h, 6h, 8h respectively denote cells without and with 1h, 2h, 4h, 6h and 8h OGD treatment. One-way ANOVA with Tukey–Kramer post hoc test. ¥P<0.05 vs other OGD group. *P<0.05 vs. control group.

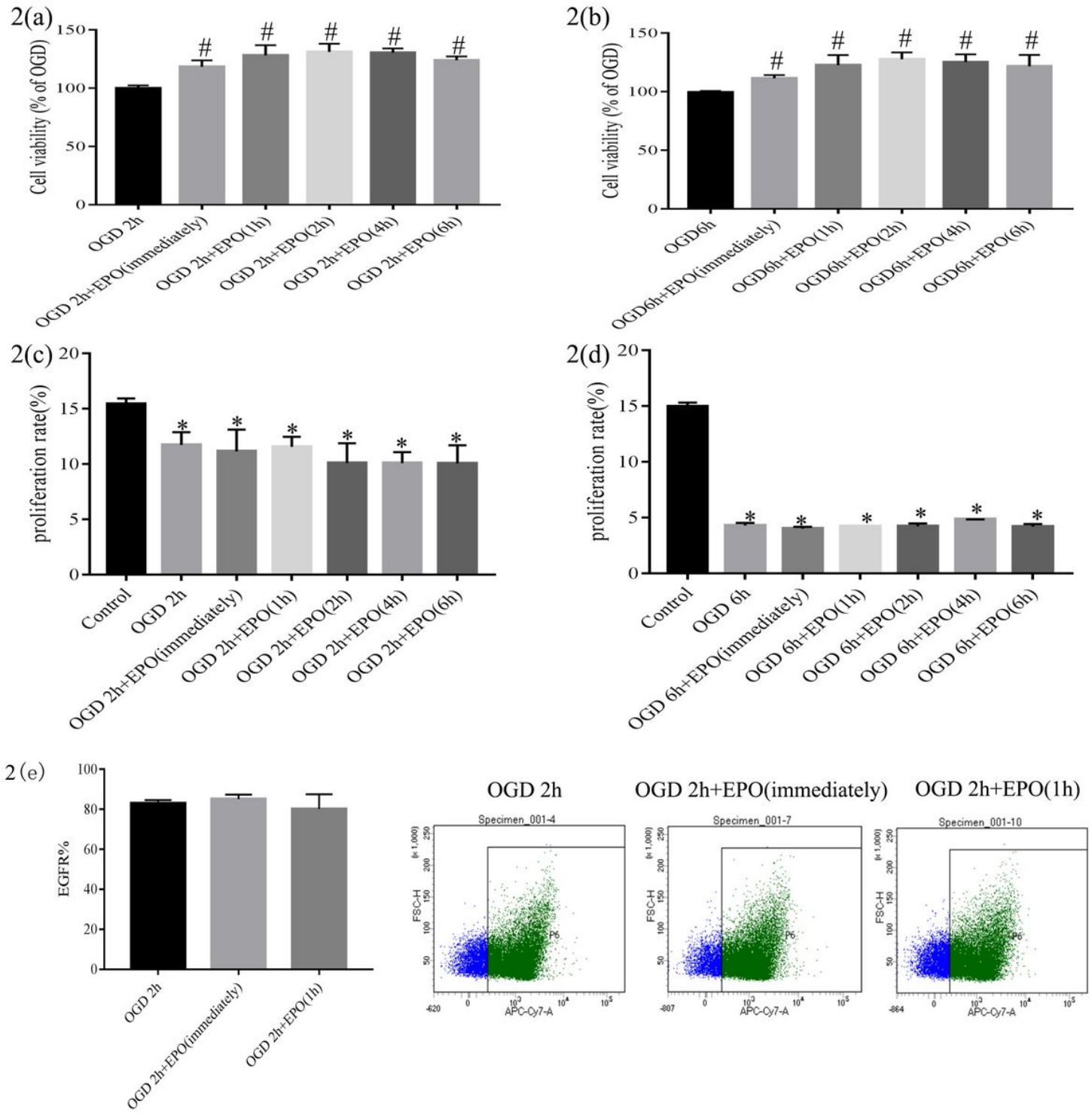

Figure 2

EPO increase the cell viability while exert no effect on proliferation of neural stem and progenitor cells. (a,b) Cell viability after 2h(a) or 6h(b) of OGD plus EPO treatment were determined by CellTiter-Glo®Luminescent assay at 2 days after OGD. (c, d) Cell proliferation rate after 2h(c) and 6h (d) of OGD plus EPO treatment were determined by Edu assay at 4 days after OGD. EPO (immediately) denotes cells were given EPO (50U/ml) immediately after OGD treatment. EPO (1, 2, 4, 6h) denotes cells were given EPO (50U/ml) 1, 2, 4, or 6h after OGD treatment. (e) EGFR% was detected by flow cytometry 1 day after 2h of OGD treament. OGD

denotes cells were not given EPO treament after OGD. EPO (immediately) denotes cells were given EPO (50U/ml) immediately after OGD treatment. EPO (1h) denotes cells were given EPO (50U/ml) 1h after OGD treatment. One-way ANOVA with Tukey–Kramer post hoc test. #P<0.05 vs. OGD group. *P<0.05 vs. control group.

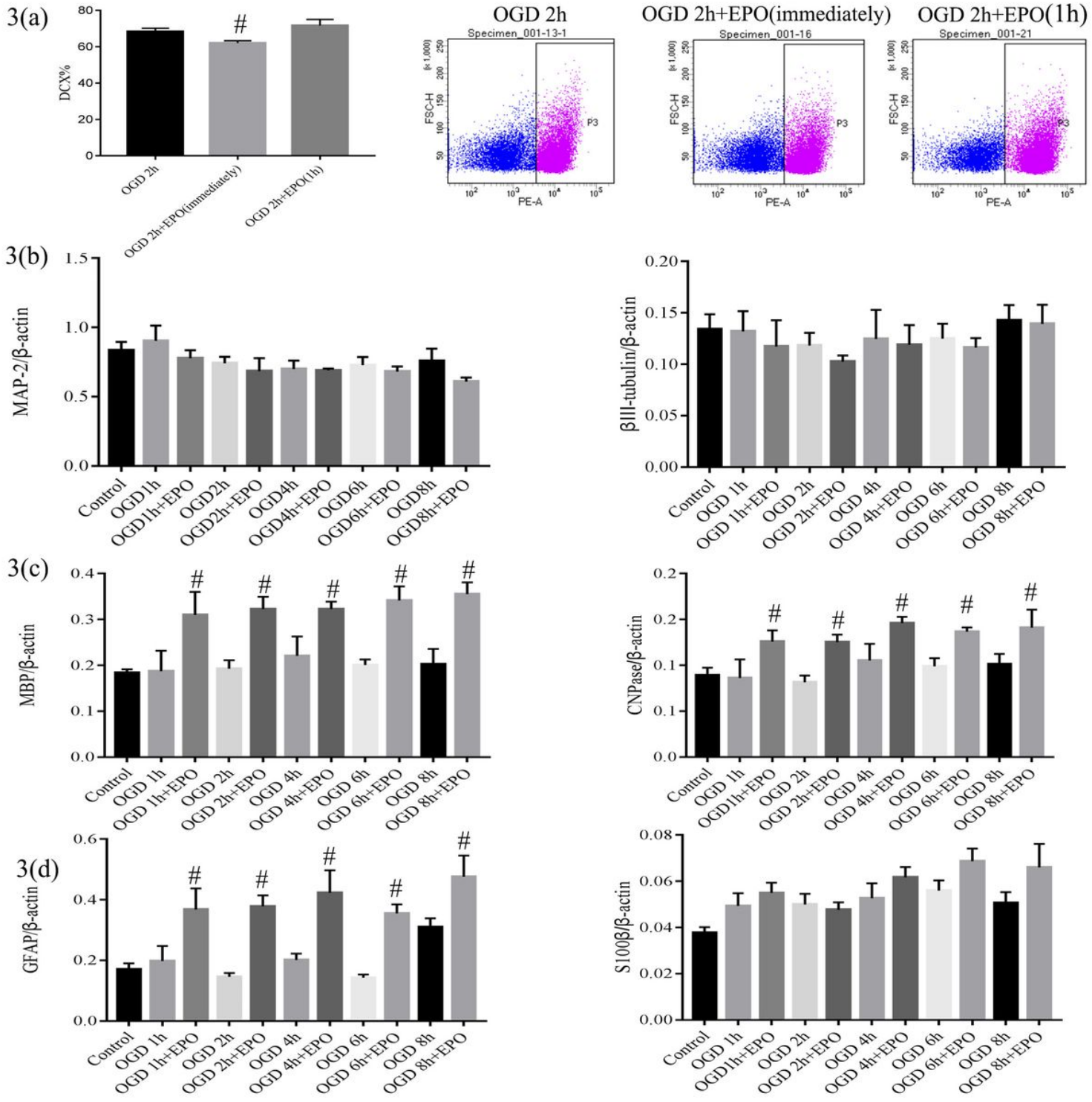

Figure 3

EPO treatment increases the differentiation of neural stem and progenitor cells towards oligodendrocytes and astrocytes at 7 day after OGD/R. (a) DCX% was detected by flow cytometry 1 day after 2h of OGD

treament. OGD denotes cells were not given EPO treament after OGD. EPO (immediately) denotes cells were given EPO (50U/ml) immediately after OGD treatment. EPO (1h) denotes cells were given EPO (50U/ml) 1h after OGD treatment. Gene expression of (b) neuronal markers MAP-2 and β□-tublin, (c) the oligodendrocyte markers MBP and CNPase, (d) astrocyte markers GFAP and S100β in different groups were determined by RT-PCR. Control denotes cells without OGD treatment. OGD 1, 2, 4, 6 and 8h denote cells were treated with 1h, 2h, 4h, 6h and 8h OGD. OGD 1, 2, 4, 6 and 8h+EPO denote cells were given 50U/ml EPO after OGD operation for 1h, 2h, 4h, 6h and 8h. One-way ANOVA with Tukey–Kramer post hoc test. #P<0.05 vs. OGD group.

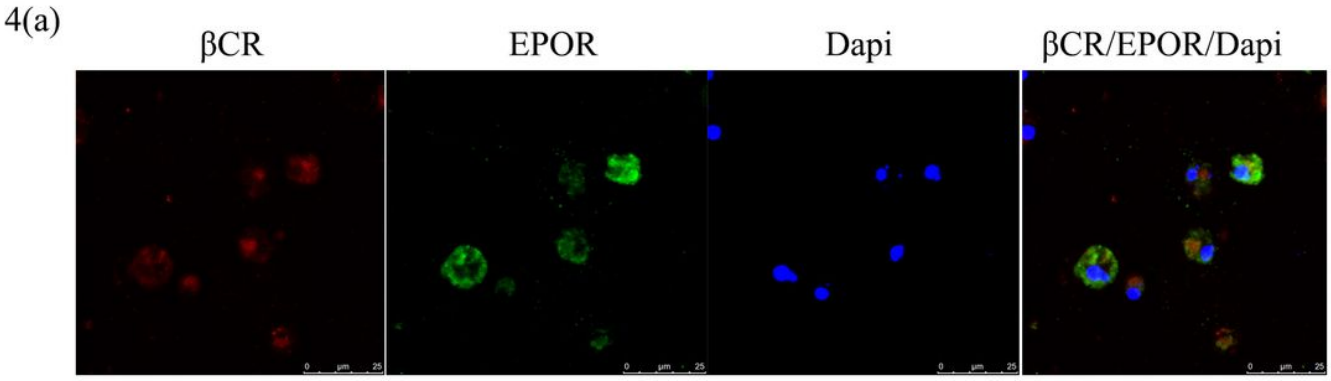

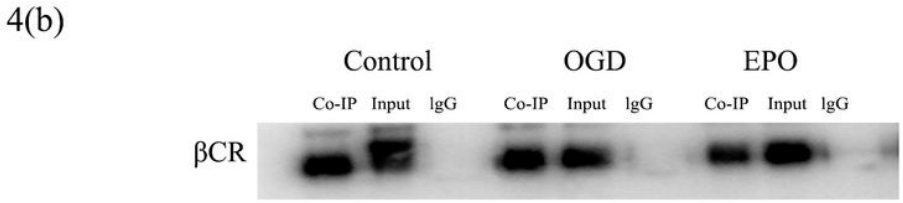

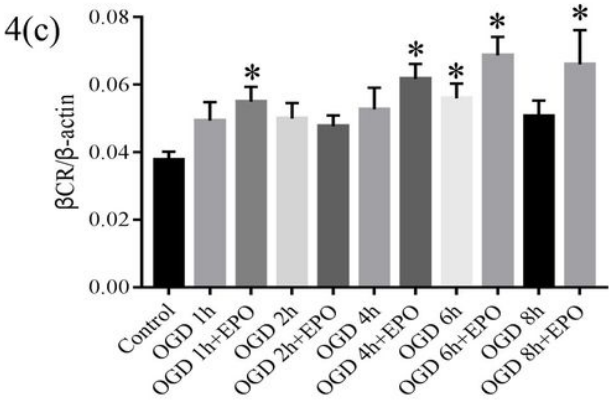

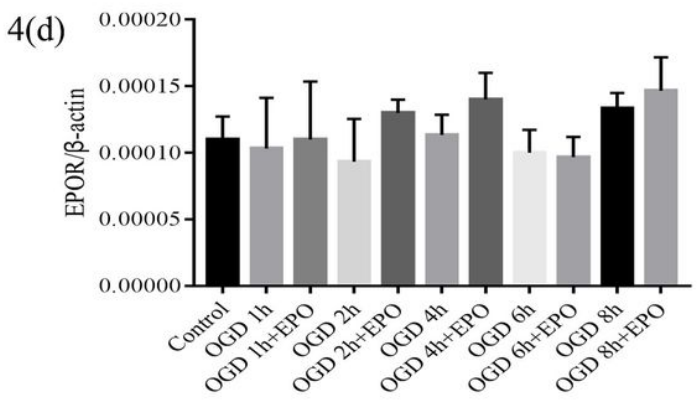

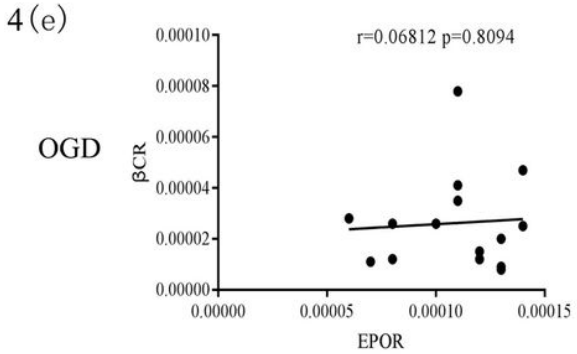

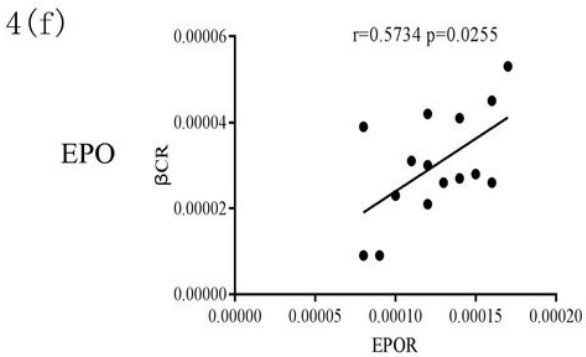

Figure 4

EPOR/βCR heterodimer exists on primary neural stem and progenitor cells. (a) Confocal microscopy was used to determine the colocalization of EPOR and βCR on neural stem and progenitor cells. Nuclei were stained with DAPI. (b) Cellular lysates immunoprecipitated (IP) with anti-EPOR Ab (Co-IP) or mouse lgGb2 (lgG) and cell lysates without IP treatment (input) were immunoprobed with anti-βCR by immunoblotting. (c, d) Gene expression of the EPOR and βCR in different groups of cells were measured by RT-PCR. Control denotes cells without OGD treatment. OGD 1, 2, 4, 6 and 8h denote cells were treated with 1h, 2h, 4h, 6h and 8h OGD. OGD 1, 2, 4, 6 and 8h+EPO denote cells were given 50U/ml EPO after OGD operation for 1h, 2h, 4h, 6h and 8h. (e, f) Correlation between βcr and Epor after OGD or plus EPO treatment. The correlation between two variables was performed using the Pearson's correlation test. One-way ANOVA with Tukey–Kramer post hoc test. #P<0.05 vs. OGD group.

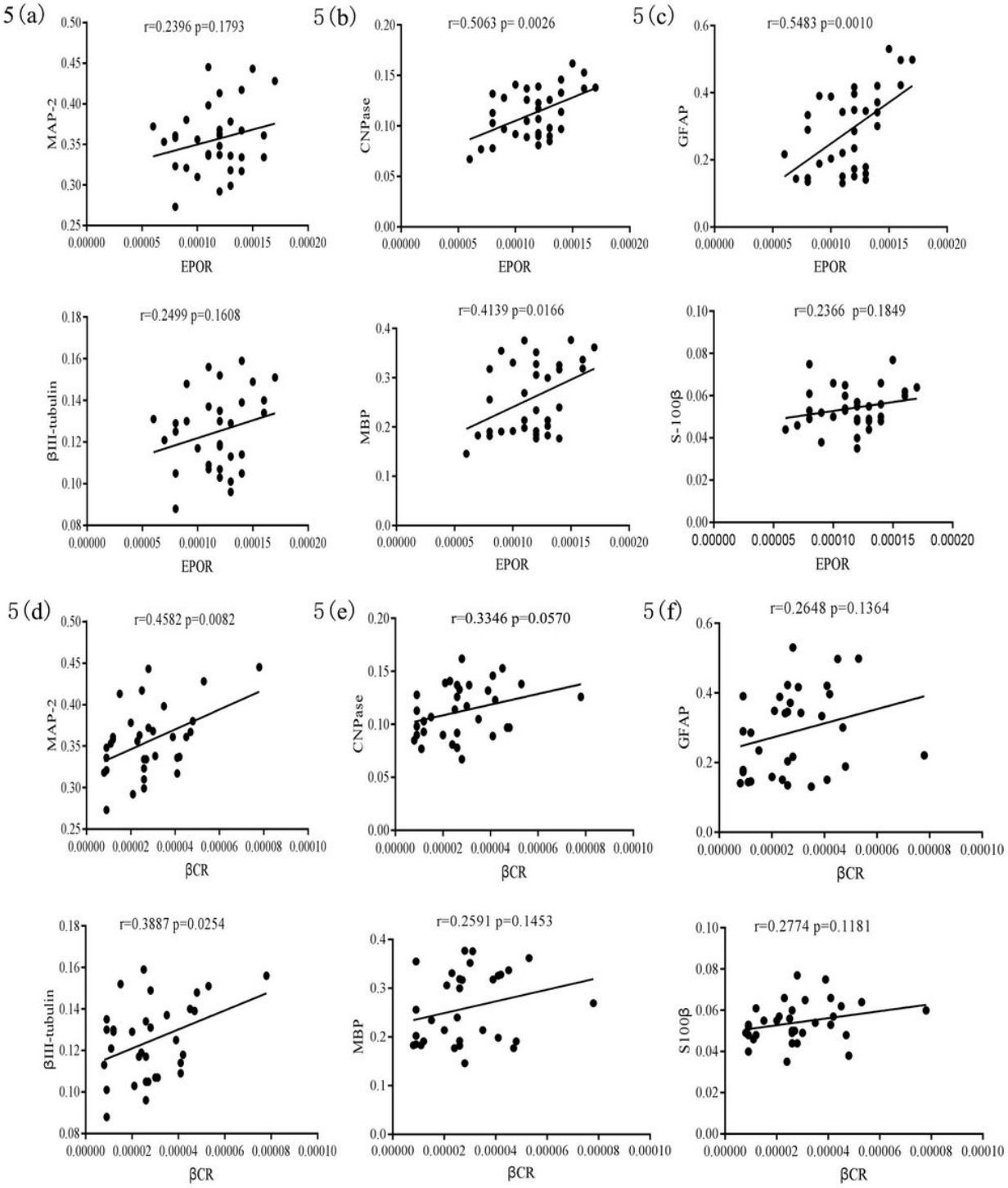

Figure 5

Correlation between EPOR/βCR and neural markers in primary neural stem and progenitor cells. (a) Correlation between EPOR and neuronal markers MAP-2 and β□-tublin. (b) Correlation between EPOR and oligodendrocyte markers MBP and CNPase. (c) Correlation between EPOR and astrocyte markers GFAP and S100β. (d) Correlation between βCR and neuronal markers MAP-2 and β□-tublin. (e) Correlation between βCR and oligodendrocyte markers MBP and CNPase. (f) Correlation between βCR and astrocyte markers

GFAP and S100β. The correlation between two variables was performed using the Pearson's correlation test.

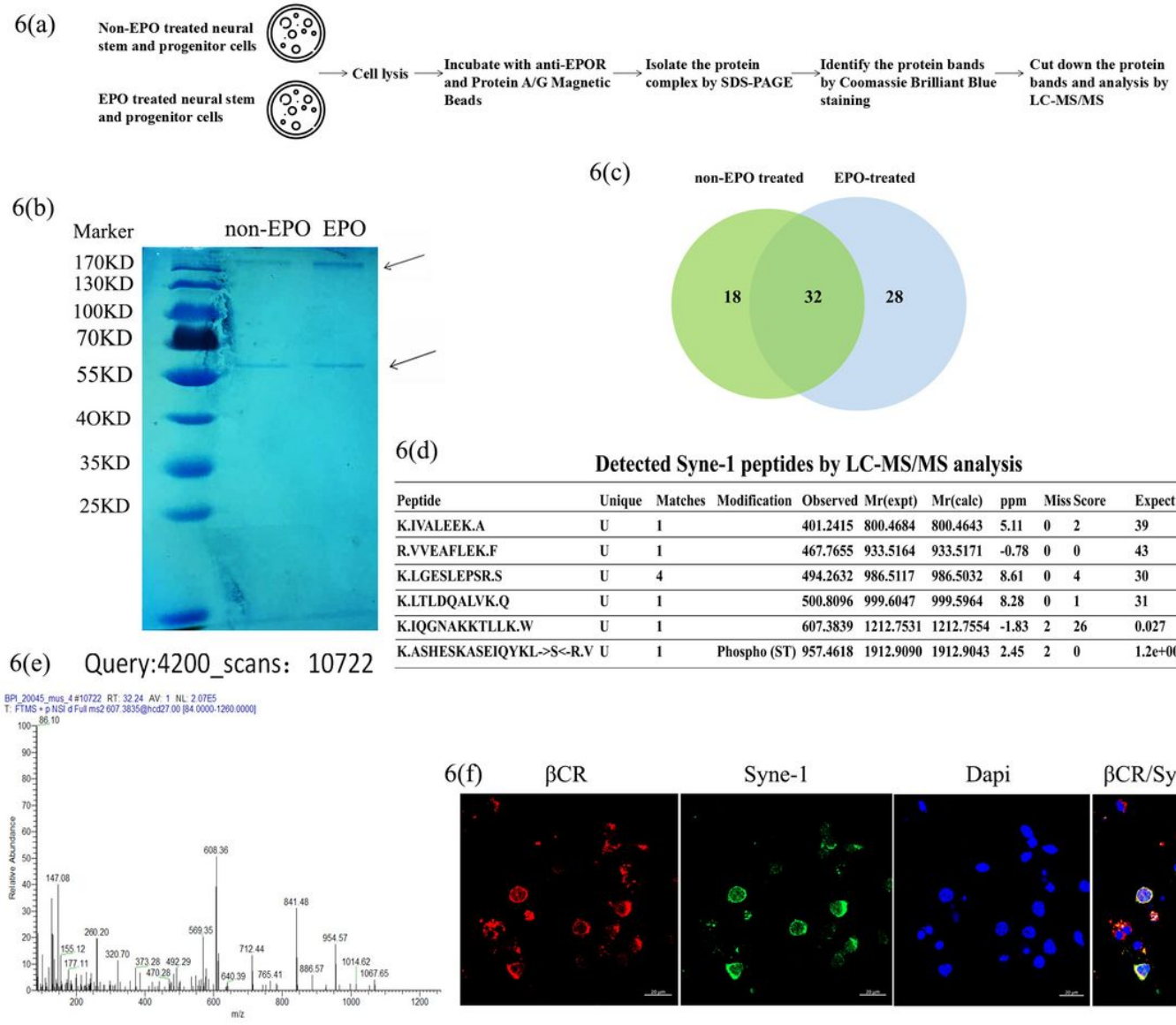

Peptide	Unique	Matches	Modification	Observed	Mr(expt)	Mr(calc)	ppm	Miss	Score	Expect	Rank	Query
K.IVALEEK.A	U	1		401.2415	800.4684	800.4643	5.11	0	2	39	6	191
R.VVEAFLEK.F	U	1		467.7655	933.5164	933.5171	-0.78	0	0	43	6	1143
K.LGESLEPSR.S	U	4		494.2632	986.5117	986.5032	8.61	0	4	30	2	1571
K.LTLDQALVK.Q	U	1		500.8096	999.6047	999.5964	8.28	0	1	31	4	1717
K.IQGNAKKTLLK.W	U	1		607.3839	1212.7531	1212.7554	-1.83	2	26	0.027	1	4200
K.ASHESKASEIQYKL->S<-R.V	U	1	Phospho (ST)	957.4618	1912.9090	1912.9043	2.45	2	0	1.2e+002	2	10673

Figure 6

Syne-1 was a downstream signaling of EPOR/βCR heteromimer on the neural stem and progenitor cells. (a) The flowcharts of LC-MS/MS analysis. (b) Coomassie brilliant blue staining of the SDS-PAGE gel. The arrowhead indicates the protein bands. (c) Venn analysis of protein bands specifically pulled down by EPOR/βCR hemerodimer from non-EPO treated and EPO-treated (EPO) neural stem and progenitor cell

lysates. (d) The table of Syne-1 peptides identified by LC–MS/MS. (e) The ion mass spectra of one matched peptide of Syne-1. (f) Primary neural stem and progenitor cells were immunostained with anti-βCR (red) and anti-Syne-1 (green) for confocal microscopy examination. Nuclei were stained with DAPI.

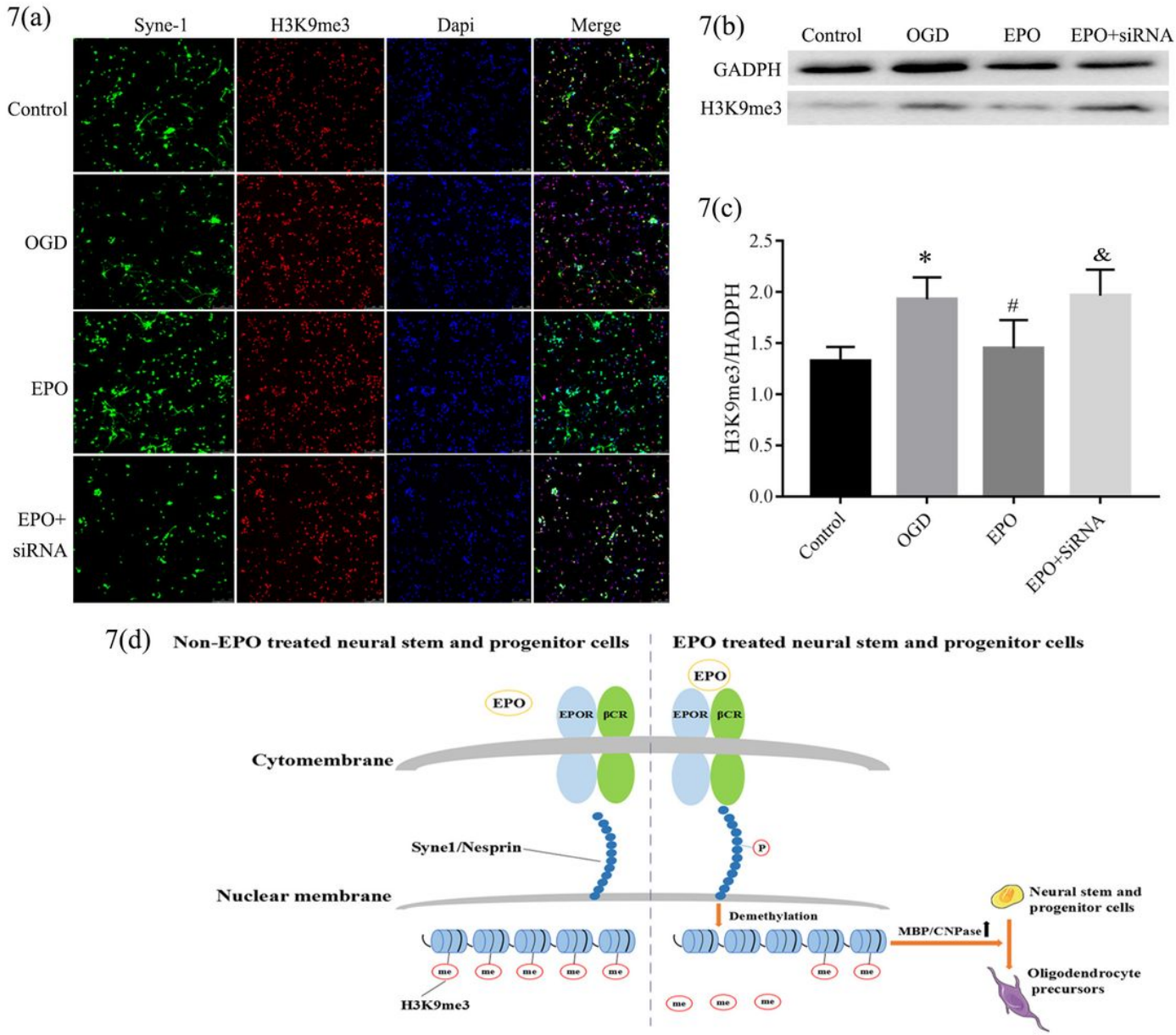

Figure 7

Syne-1/H3K9me3 signaling pathway mediated the effect of EPO through EPOR/βCR heteromimer in primary neural stem and progenitor cells. (a) Confocal microscopy was used to determine the colocalization of Syne-1 and H3K9me3. Nuclei were stained with DAPI. Cells were treated with βCR siRNA for 48h and were then treated with EPO (50U/ml) immediately after OGD. (b, c) Protein expression level of H3K9me3 was assessed by western blot. N=4/group. One-way ANOVA with Tukey–Kramer post hoc test. *P<0.05 vs. control group. #P<0.05 vs. OGD group. &P<0.05 vs. EPO group. (d) The diagram to elucidate a possible mechanism of how EPO activates the βCR/Syne-1/H3K9me3 pathway and improves the differentiation of neural stem cells into oligodendrocytes.